Available online at www.sciencedirect.com
SCIENCE DIRECT
Journal of Catalysis 229 (2005) 119–126
JOURNAL OF CATALYSIS
www.elsevier.com/locate/jcat

Effect of the Si/Al ratio on the structure and surface properties of silica-alumina-pillared clays

A. Gil [a,*], M.A. Vicente [b], S.A. Korili [a]

[a] *Departamento de Química Aplicada, Edificio Los Acebos, Universidad Pública de Navarra, Campus de Arrosadía, s/n, E-31006 Pamplona, Spain*
[b] *Departamento de Química Inorgánica, Facultad de Ciencias Químicas, Universidad de Salamanca, Plaza de la Merced, s/n, E-37008 Salamanca, Spain*

Received 18 August 2004; revised 15 October 2004; accepted 18 October 2004

Available online 26 November 2004

Abstract

In the present work, the synthesis of silica-alumina-pillared montmorillonites and their structure are studied. Hydroxy-silico-aluminum oligocations have been obtained by treating previously synthesised aluminum polycations with $Si(OC_2H_5)_4$. Several Si/Al ratios (0, 0.5, 1, and 2) have been used to prepare pillared clays with various microporous accessibility and acidic properties. The study of the fractal dimensions of the solids shows that their surface becomes more heterogeneous after pillaring. The acidity of alumina- and silica-alumina-pillared montmorillonites is mainly of the Lewis type, and the nature of the acid sites detected by pyridine adsorption seems to be independent of the Si/Al ratio. These results are supported by the product distribution obtained in the 1-butanol dehydration reaction.

Keywords: Silica-alumina-pillared clay; Nitrogen adsorption; Micropore-size distribution; Acidity characterisation; 1-Butanol dehydration

1. Introduction

The physical and chemical properties of clay materials can be modified by acid and base activation and, in the case of layered clays, by intercalation of metallic polycations into their interlayer region. The latter process is characterised by the generation of a new porous structure and by the creation of active sites (acid and/or metallic), which can improve the behaviour of these materials.

In the last four decades, the development of inorganic pillared interlayered clays (in short PILCs), an important category of microporous materials, has created remarkable new opportunities in the field of the synthesis and applications of clay-based solids [1–5]. These materials are prepared by exchanging the charge-compensating cations present in the interlamellar space of the swelling clays with hydroxy-metal polycations. On calcining, the inserted polycations yield rigid, thermally stable oxide species, named *pillars*, which prop apart the clay layers and prevent their collapse. This process results in an interesting two-dimensional porous structure of molecular dimensions.

The microstructure developed in the pillaring process, in particular the micropore size distribution (MPSD), determines and limits the potential use of the materials in catalytic, purification, and sorption-based separation processes. Therefore, the characterisation and quantitative evaluation of the microstructure are the objects of a considerable research effort [6–14], in which experimental and theoretical studies based on gas adsorption are the approach most widely considered. Other techniques (calorimetry, electron microscopy, nuclear magnetic resonance, etc.) have also proved to be very useful in the investigation of the microstructure of PILCs.

The intercalation of clays with solutions containing two or more metallic cations has been widely studied [3]. Usually, one of the cations polymerises easily, and it makes up the majority of the mixture, and the addition of small molar fractions of a second cation is intended to improve the thermal and catalytic properties of the final solids. Mixed

* Corresponding author.
E-mail address: andoni@unavarra.es (A. Gil).

0021-9517/$ – see front matter
doi:10.1016/j.jcat.2004.10.013

systems, such as Ga–Al, Ln–Al, Si–Al, Fe–Al, Cr–Al, Zr–Al, and Si–Ti, among others, have been reported in the literature. The use of hydroxy-silico-aluminum oligocations as pillaring agents is particularly interesting, considering that the initial objective of pillared clay research was to prepare materials as alternatives to zeolites, since clays pillared with Si–Al oligomers may have a chemical composition very similar to that of zeolites. The intercalation of clays with the use of oligocations of this type has been reported by several authors [15–23].

Another important question in the studies dealing with the pillaring process of clays is the acidity of these materials. The total acidity and the type of acid sites (Brønsted and Lewis) depend on several factors, such as the exchanging cations, the preparation method, and the nature of the starting clay [24–27]. The Lewis acidity in alumina-pillared montmorillonites is due to two types of sites, both ascribable to aluminum centres [28] that are related to aluminum sites in the tetrahedral layer of the clay and to aluminum sites on pillars [25,29]. In the same way, several sources for Brønsted acidity have been discussed in the literature: (i) the structural hydroxyl groups in the clay layer from the initial sites of ion exchange [25]; (ii) the protons derived from the cationic oligomers, which, upon heating, decompose into metal oxide pillars and liberate protons [24,30]; and (iii) synergy between the siliceous clay sheet and the pillar [28,31].

The aim of this work is to contribute to the evaluation of the surface properties and the microstructure developed by silica-alumina-pillared clays.

2. Experimental

The starting material, Na-montmorillonite Kunipia F from the Kunimine Co., was dispersed as received in water, aged, and washed by dialysis until the conductivity of the surrounding water was less than 1.5 μS. The solid content of the dialysed clay dispersion was 7–10 g/l. This clay was submitted to intercalation with pure Al polycations and with mixed Al–Si polycations. Pure aluminum polycation solution [32,33] was prepared by slow titration of a 0.2 M solution of $AlCl_3 \cdot 6H_2O$ (Merck, PA) with a 0.2 M solution of NaOH (Panreac, PA) under vigorous stirring, with a OH^-/Al^{3+} mole ratio equal to 2. The hydrolysed solution was allowed to age for 48 h at room temperature under continuous stirring (pH = 4.06). The hydroxy-silico-aluminum solutions were prepared by the reaction of various amounts of tetraethylorthosilicate, $Si(OC_2H_5)_4$ (Aldrich, 99.999%), with the aluminum solution (Si/Al mole ratios of 0.5, 1, and 2) for 24 h [23]. We carried out the intercalation process by dropping the clay suspensions into the hydroxy-silico-aluminium solutions under vigourous stirring, using an Al^{3+}/clay ratio of 11 mM/g. The solids were kept in contact with the solution at room temperature for 24 h, washed by centrifugation, dried at 393 K for 16 h, and calcined at various temperatures for 4 h to obtain the silica-alumina-pillared montmorillonites. The samples are referred to as SiAl-number, the number indicating the Si/Al intercalation ratio used (0.0 for the pure Al solution).

The solids were characterised by X-ray diffraction (XRD) analysis, N_2 adsorption at 77 K, and FTIR analysis of adsorbed pyridine. In XRD analysis, a thin layer of the clays on glass slides was examined on a Phillips PW 1710 diffractometer with Ni-filtered Cu-K_α radiation. Nitrogen adsorption experiments were performed at 77 K with use of a static volumetric apparatus (Micromeritics ASAP2000 adsorption analyser). The samples were previously degassed at 393 K for 24 h. Nitrogen adsorption data were obtained with the use of 0.1 g of sample and successive doses of nitrogen of 0.5 cm^3/g measured at STP conditions until $p/p^0 = 0.04$ was reached. Subsequently, further nitrogen was added and the volume required to achieve a fixed set of p/p^0 was measured. Only the nitrogen adsorption data up to a relative pressure of 0.2 were considered in the micropore characterisation. FT-IR spectra were recorded with a Brücker FT 88 spectrometer. Samples were calcined at 773 K before analysis. In preparation for pyridine adsorption, samples were pressed into self-supported disks, placed in an IR cell, and treated under vacuum (1.33×10^{-4} Pa) at 673 K for 4 h. After cooling to room temperature, a spectrum was recorded. The samples were then exposed to pyridine vapour for 5 min. After evacuation (6.67×10^{-3} Pa) at various temperatures for 1 h, the corresponding spectra were recorded.

The 1-butanol dehydration reaction was carried out in a tubular fixed-bed Pyrex glass reactor at 523 K and atmospheric pressure. Before reaction, the solids were sieved and a particle size fraction of 100–200 μm was used. Solid activation was performed in helium flow, 100 cm^3/min, at 673 K for 1 h. The catalytic experiments were performed at a W/F_{in} ratio of 10 $g\,h/mmol_{1\text{-butanol}}$. To prevent the condensation of 1-butanol or of the reaction products, all lines from the saturator to the chromatograph were heated to 373 K. On-line analysis of the product stream was performed on a Shimadzu GC-8A gas chromatograph. A 20% Reoflex/400 Embacel column was used to separate and quantify the 1-butanol and the dehydration products, butyraldehyde and dibutylether. 1-Butene and the isomerisation products, *cis*- and *trans*-2-butene, were analysed with a 2-m Octane/Porasil column. The conversion was defined as the ratio of the amount of converted 1-butanol to the amount of 1-butanol supplied at the reactor inlet. The selectivity to each product was defined as the mole ratio of the reacted 1-butanol that was converted into a given product.

3. Results and discussion

The intercalation of layered clays yields a two-dimensional porous structure of molecular size characterised by the distance between the clay layers (*interlayer spacing*), and the distance between the intercalating species (*interpillar spacing*). The interlayer spacing can be estimated from the

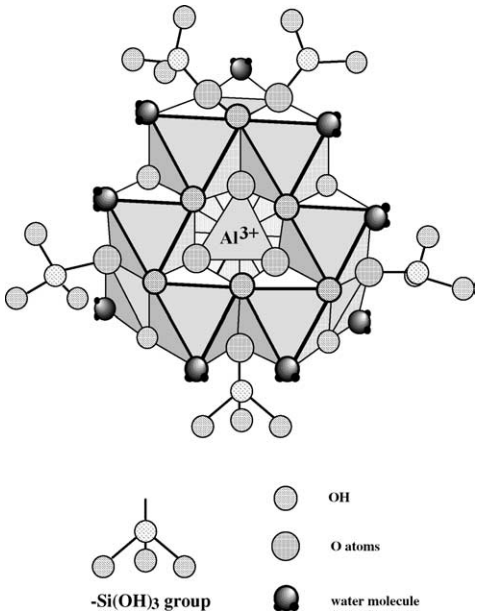

Fig. 1. Molecular model of a hydroxyl-silico-aluminum oligocation derived from $[Al_{13}O_4(OH)_{24}(H_2O)_{12}]^{7+}$ by partial substitution of hydrogen atoms from OH groups by $–Si(OH)_3$ groups.

basal spacing $d(001)$ of the samples. The interpillar spacing is more difficult to determine. The most commonly used procedure is to obtain the adsorption isotherm from experimental results at very low relative pressures and then apply a suitable model to interpret the data in terms of pore sizes.

The basal spacings of the pillared solids prepared in this work and treated at various temperatures between 298 and 673 K varied between 1.76 and 1.35 nm (see Table 1). The basal spacing of the SiAl-0.0 solid fit well, as expected, with the values generally reported in the literature for clays intercalated and pillared with the Al_{13} polycation [3]. The addition of low amounts of Si gives solids with similar basal spacings, thus indicating that the height and the thermal resistance of the hydroxy-silico-aluminium intercalated species is similar to that of Al_{13} polycations. However, in the solid SiAl-2.0, which had the highest Si/Al ratio studied, the basal spacing of 1.59 nm indicated that the solid was not successfully intercalated. In all cases, the basal spacings of the samples decreased with increasing calcination temperatures and increasing Si/Al mole ratio, as usually reported for the transformation from the intercalating polycations to the final pillars.

The basal spacing of the solids can be explained by the chemistry in solution of the cations participating in intercalation. For sample SiAl-0.0, optimal conditions for the polymerisation of Al^{3+} to form Al_{13} oligomers were chosen, and this polycation can be expected to form a majority of the product. When tetraethylorthosilicate is added, the strong affinity of Si(IV) for hydroxyl groups may allow the formation of $Si(OH)_4$ units. For SiAl-0.5 and SiAl-1.0 samples, these units can bond to Al_{13} oligomers, but without significantly altering their polymerisation process, that is, without provoking their depolymerisation, such that the intercalation is similar to that observed with pure Al_{13} polycations. However, when the amount of Si increases (sample SiAl-2.0), the amount of OH^- required for silicium increases, Al_{13} polycations are destroyed, and, subsequently, the clay is not intercalated. The situation described for samples SiAl-0.5 and SiAl-1.0 has been reported in the literature [20,34]. $Si(OH)_4$ units are able to react with OH groups from the pillars, giving rise to $Si(OH)_3$ moieties placed in the lateral parts of the Al_{13} oligomers (see Fig. 1). Two simple formulations will be possible for this reaction [34], and they can be expressed in terms of cations and hydroxyls as follows:

$$[Al_{13}(OH)_{32}(H_2O)_8]^{7+} + Si(OH)_4 \rightarrow [Al_{13}Si(OH)_{36}(H_2O)_8]^{7+}$$

or

$$[Al_{13}(OH)_{32}(H_2O)_8]^{7+} + Si(OH)_4 \rightarrow [Al_{13}Si(OH)_{37}(H_2O)_6]^{6+} + (H_3O)^+.$$

With both formulations (more easily with the first one), it is immediately deduced that for 7+ polycations, the ratio OH/metal is 2.46 for the pure Al polycation and 2.50 for the mixed Al–Si polycation, when only one Si atom is incorporated to the oligomeric structure. Considering the possible coordination of the metallic cation with water or hydroxyls, and the transformation between these species, it is obvious that the incorporation of Si into Al_{13}-polycations implies an increase in OH/metal ratio if the charge of the polycation is supposed to be constant (or, alternatively, an increase in the charge of the polycation may be observed). As indicated, the height of the intercalating polycations/pillars is similar when they are based on Al_{13} units, independently of the incorporation of Si moieties. However, the diameter of the polycations/pillars may be considerably different from one solid to another. As indicated, the addition of tetraethylorthosilicate to Al_{13} solutions produces the progressive incorporation of $–Si(OH)_3$ units into lateral positions of the polycations, by

Table 1
Evolution of the basal spacings and the fwhm indexes of the (001) reflection peak of the samples with the thermal treatment

Sample	298 K		473 K		573 K		673 K	
	$d(001)$ (nm)	fwhm	$d(001)$ (nm)	fwhm	$d(001)$ (nm)	fwhm	$d(001)$ (nm)	fwhm
SiAl-0.0	1.76	2.8689	1.73	2.3221	1.66	2.6034	1.56	2.1880
SiAl-0.5	1.72	2.8076	1.72	2.4839	1.59	2.6936	1.54	2.7285
SiAl-1.0	1.72	2.6352	1.66	2.3855	1.47	2.4273	1.43	2.4110
SiAl-2.0	1.59	1.8574	1.51	2.0082	1.43	1.9403	1.35	1.8166

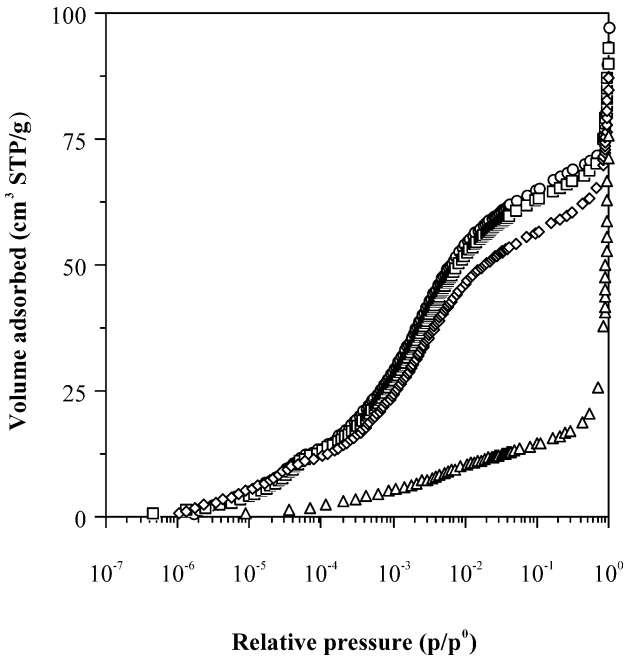

Fig. 2. Nitrogen adsorption at 77 K, in semilogarithmic plot, starting from very low pressures: (○) SiAl-0.0, (□) SiAl-0.5, (◇) SiAl-1.0, (▽) SiAl-2.0.

bonding to oxygen atoms (see Fig. 1) [3]. This lateral disposition of these units may provoke a strong blockage of the porosity of the solids, which may be more significant for the intercalated solids than for the calcined ones, when these units may be transformed into very small SiO_2-like particles situated on the surface of Al_2O_3-like pillars or integrated into the pillars forming Si–Al mixed oxide particles.

The nitrogen adsorption of the samples starting from very low pressures is shown in Fig. 2. The adsorption isotherms were of type I in the Brunauer, Deming, Deming, and Teller (BDDT) classification [35]. The Langmuir surface area (S_{Lang}) was calculated from adsorption data in the relative pressure range between 0.01 and 0.05, for a nitrogen molecule cross-sectional area of 0.160 nm^2 [35]. The total pore volume (V_{p}) was assessed from the amount of nitrogen adsorbed at a relative pressure of 0.98, assuming that the density of the nitrogen condensed in the pores is equal to that of liquid nitrogen at 77 K (0.81 cm^3/g) [35]. Differences were found in the surface areas (289–86 m^2/g) and total pore volumes (0.163–0.144 cm^3/g) of the samples treated at 673 K for 4 h, depending on the Si/Al mole ratio; these magnitudes decreased when the Si/Al ratio was increased.

Several methods and models have been applied to the nitrogen adsorption data for various pore geometries to characterise the microporosity of the solids [13,36,37]. The surface properties and the accessibility to the micropores affect these approaches. There are still uncertainties about which of these models works better for pillared materials and how to interpret the pore size distributions obtained, mainly because of the influence of surface factors [10,11,38]. Although it can be assumed that the clay sheets are parallel to each other, the interconnecting pillars are relatively closely spaced, so the resulting pores may be more cylindrical than slit-like. Nevertheless, it has been reported that the slit-like geometry gives a reasonable description of the complicated microporous structure of PILCs [7,10], but these studies have usually been carried out on Al-PILCs. In the present work, the micropore size distributions (MPSD) derived from the models proposed by Horvath and Kawazoe [39] (HK), Cheng and Yang [8] (ChY), and Saito and Foley [40] (SF) have been used to study the microporous region of the solids. The physicochemical properties of the adsorbate-adsorbent system required by these models were estimated as proposed by Gil and Grange [10]. A comparison of the MPSD derived from these models for the samples is shown in Fig. 3. As can be seen, the distributions are bimodal and do not depend much on the model. It seems that the microstructure of these materials can be equally described by either slit-like or cylindrical pore geometries when nitrogen is used as the adsorbate [13]. When the MPSDs for SiAl-0.0, SiAl-0.5, and SiAl-1.0 are compared, no differences are observed. The distributions show a first maximum at about 0.54 nm, a shoulder at about 0.64 nm, and a second maximum at 0.72 nm. The distribution for sample SiAl-2.0 shows the lower microporosity values of the series, in agreement with the absence of expansion of the layers in these solids observed by XRD. The microporous volumes ($V_{\mu\mathrm{p(HK)}}$), calculated according to the HK model and with the method proposed by Gil and Grange [10], and the maxima of the MPSD are summarised in Table 2. For comparison purposes, the microporous volumes have been also calculated by means of the Dubinin–Astakhov (DA) equation [41] in the relative pressure range between 0.01 and 0.05 ($V_{\mu\mathrm{p(DA)}}$); the results are also included in Table 2.

Maximum pore diameters at 0.55 and 0.66–0.68 nm have been obtained for the samples when the Jaroniec–Gadkaree–Choma model (JGC) is considered [42] (see Fig. 4). The differences observed with respect to the MPSD presented in Fig. 3 can be related to the fact that the JGC model provides an overall description of the adsorption process, whereas the methods based on the HK model depend on the adsorbent-adsorbate interaction potential, which results in an important contribution of the smallest pores.

The fractal dimensions (D) of the samples calculated from the method proposed by Avnir and Jaroniec [43] in the range of relative pressures between 0.08 and 0.20 [44] are also presented in Table 2. The fractal dimension, which quantitatively evaluates the fractal geometry [45], is a measure of the surface and structural irregularities of a solid. The value of this dimension can vary from 2 to 3 [46]. The lower limiting value of 2 corresponds to a perfectly regular smooth surface, whereas the upper limiting value of 3 relates to the maximum allowed complexity of the surface. In addition to the surface heterogeneity, the structural heterogeneity can contribute significantly to the fractal dimension. The surface heterogeneity results from the presence of functional groups and impurities, whereas the structural heterogeneity arises from networking effects related to in-

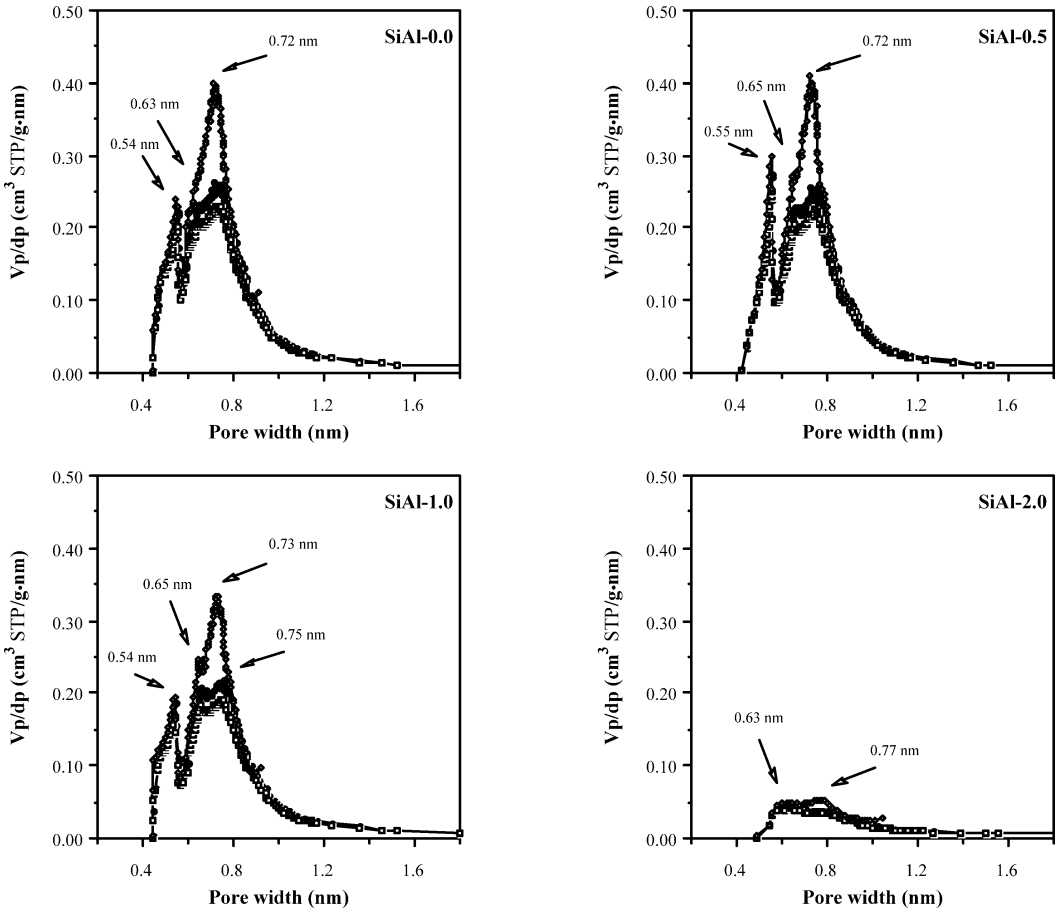

Fig. 3. Comparison of the micropore-size distributions derived from Horvath–Kawazoe (slit-like, ●), Saito–Foley (cylindrical, □) and Cheng–Yang (slit-like, ◇) pore models.

terconnected pores of various sizes and shapes and from the presence of various crystallographic and surface irregularities. The values obtained for the solids prepared in this study are very close to the upper limiting value of 3, thus indicating a significant contribution of the structural and/or surface heterogeneity in accordance with the results discussed previously. The *D* values of the SiAl-0.0, SiAl-0.5, and SiAl-1.0 samples are very similar, 2.89–2.90, indicating a high structural similarity between these three samples. However, the SiAl-2.0 sample has a clearly lower *D* value, 2.72, reflecting that this sample has a surface that is significantly different and less heterogeneous from a structural point of view. As seen previously, this sample is not intercalated, and the absence of expanded layers with a network of pillars between them is reflected as a decrease in *D* values. The *D* value for unpillared Kunimine montmorillonite is 2.60 [44]. So, intercalation clearly induces heterogenisation of the structure and/or surface.

Table 2
Microporous properties derived from the nitrogen adsorption at 77 K of the samples indicated

Sample	Slit-like model			JGC model	DA equation			
	$V_{\mu p(HK)}$[a] (cm^3/g)	dp_{HK}[b] (Å)	dp_{ChY}[c] (Å)	dp_{JGC}[d] (Å)	$V_{\mu p(DA)}$[a] (cm^3/g)	E[e] (kJ/mol)	n[f]	D[g]
SiAl-0.0	0.105	5.7–11.7	5.7–8.9	0.55; 0.64	0.107	20.9	2.0	2.90
SiAl-0.5	0.101	5.7–11.7	5.7–8.9	0.55; 0.68	0.105	20.6	2.0	2.90
SiAl-1.0	0.091	5.7–11.7	5.7–8.9	0.54; 0.68	0.097	21.2	1.7	2.89
SiAl-2.0	0.025	4.9–12.2	4.9–9.9	0.66	0.025	15.9	1.9	2.72

[a] Specific micropore volumes derived from Korvath–Kawazoe (HK) model and Dubinin–Astakhov (DA) equation.
[b] Pore diameter range of the second maximum of the Horvath–Kawazoe micropore size distributions.
[c] Pore diameter range of the second maximum of the Cheng–Yang micropore size distributions.
[d] Maxima of Jaroniec–Gadkaree–Choma (JGC) micropore size distributions.
[e] Characteristic energy from Dubinin–Astakhov equation.
[f] Exponent of Dubinin–Astakhov equation.
[g] Fractal dimensions calculated from Avnir–Jaroniec method in the relative pressure range 0.08–0.2.

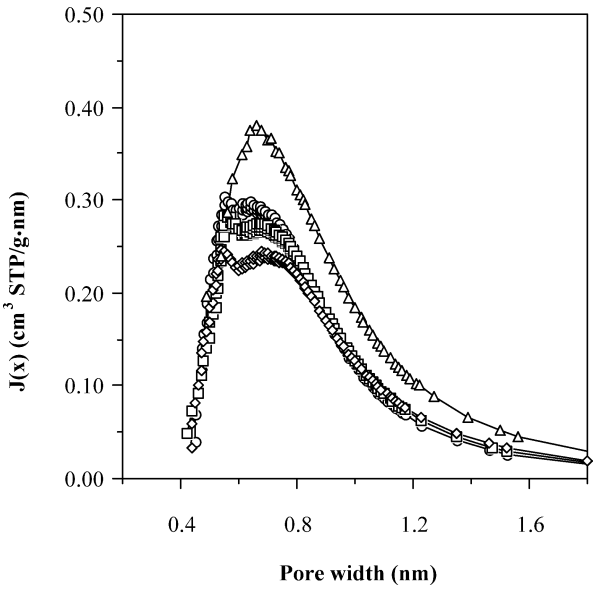

Fig. 4. Micropore-size distributions derived from the Jaroniec–Gadkaree–Choma model. (○) SiAl-0.0, (□) SiAl-0.5, (◇) SiAl-1.0, (▽) SiAl-2.0.

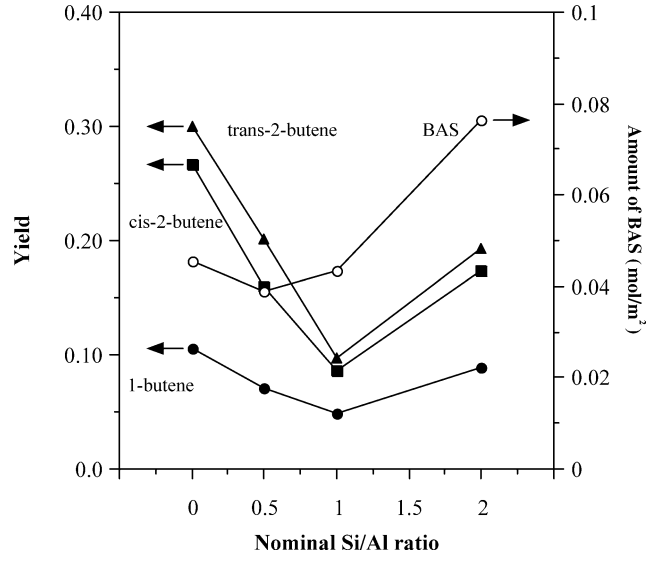

Fig. 5. Evolution of the yield to the reaction products and the amount of Brönsted acid sites (BAS) with the nominal Si/Al ratio. (●) 1-butene, (■) cis-2-butene, (▲) trans-2-butene, (○) BAS.

The specific absorption bands of chemisorbed pyridine in the 1700–1400 cm^{-1} wavenumber range have been used to distinguish between Brønsted and Lewis acid sites. Qualitatively, the pyridine adsorption spectra exhibited the same behaviour with the outgassing temperature for alumina- and silica-alumina-pillared montmorillonites. The spectra of pyridine adsorbed on silica-alumina-pillared montmorillonites after degassing at room temperature (not shown) exhibit Brønsted [47], PYH^+, bands at 1540, 1491, and 1638 cm^{-1}; Lewis acid sites, PYL, at 1448, 1617, and 1491 cm^{-1}; and physisorbed or hydrogen-bonded pyridine, HPY, at 1597 cm^{-1}. The HPY band at 1597 cm^{-1} disappears after evacuation at 423 K. There was no evidence of Brønsted acidity after outgassing above 523 K. The bands at 1623 and 1456 cm^{-1}, characteristic of Lewis acidity, were still observed even after outgassing at 673 K. The Lewis acid strength and adsorbed pyridine behaviour at various outgassing temperatures remained unchanged when silicon was added to the initial aluminium solution. The nature of the acid sites detected by pyridine adsorption in silica-alumina-pillared montmorillonites is independent of the Si/Al ratio. From these results, the acidity of alumina- and silica-alumina-pillared montmorillonites seems to be mainly of the Lewis type.

The concentrations of Brønsted and Lewis acid sites were determined from the intensities of PYH^+ and PYL bands, from the band integral area and the wafer density, and the extinction coefficients obtained by Datka et al. for the bands close to 1540 and 1450 cm^{-1} [48]. The results indicated that the Lewis acidity was predominant in all samples. The intensity of the Lewis acidity bands decreased with increasing silicon content. The intensity of Brønsted acid sites shows the same trends as observed for Lewis acidity.

The dehydration of 1-butanol is a reaction used as a probe of the acid-base properties of several oxide catalysts [49–58], mainly to detect small changes in the nature of the acid sites, their strength, and their concentration per unit surface area. The reaction can proceed through various paths: the intramolecular dehydration of 1-butanol to 1-butene, the consecutive isomerisation of 1-butene to *cis*/*trans*-2-butene, the intermolecular dehydration of two molecules of 1-butanol to dibutylether, and the direct dehydrogenation of 1-butanol to butyraldehyde. The dehydration of 1-butanol takes place via the formation of a carbonium ion, indicating that the catalytic active centres under the reaction conditions are the acid sites. The consecutive isomerisation of 1-butene to *cis*/*trans*-2-butene is often used to test the acid or basic character of catalysts. It occurs through either acid or basic catalysis; a high *cis*/*trans* ratio is observed for the base-catalysed isomerisation [59], in contrast to the value close to 1 for an acid-catalysed isomerisation [60]. Finally, the formation of dibutylether requires the cooperation of acid and basic surface sites, since this product is not formed on a very acid or a very basic oxide. Furthermore, it has to be taken into account that the intramolecular dehydration of 1-butanol to 1-butene can occur through various mechanisms (E1, E2, or E1cB; -cB, conjugated Base) [50]. To determine which mechanism is effective, Noller et al. [61] have suggested the study of the 1-butene and 2-butene distributions in reaction products. Thus, when 1-butene isomerises rapidly to 2-butene, the major reaction product, with a *cis*/*trans* ratio close to 1, an E1 mechanism is proposed.

The evolution with time on-stream of the overall 1-butanol conversion and the selectivities to the reaction products yielded by our samples were constant after 3 h on-stream. Under the reaction conditions employed, mainly butenes were detected. 1-Butene obtained from 1-butanol

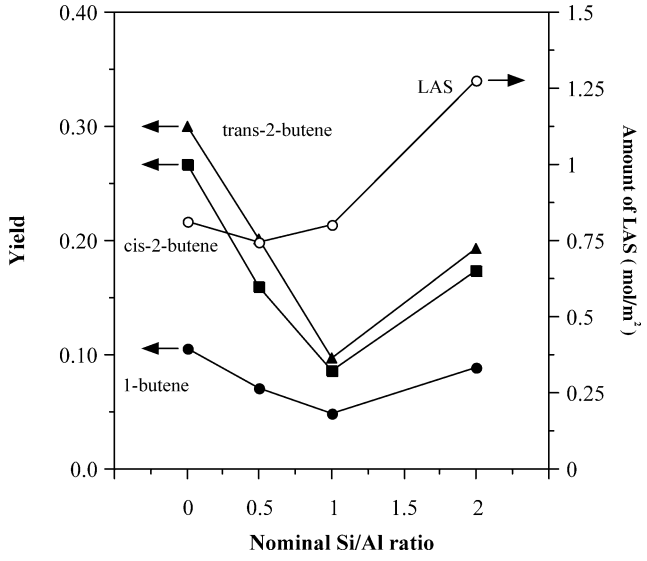

Fig. 6. Evolution of the yield to the reaction products and the amount of Lewis acid sites (LAS) with the nominal Si/Al ratio. (●) 1-butene, (■) cis-2-butene, (▲) trans-2-butene, (○) LAS.

dehydration is partially isomerised to *cis*- and *trans*-2-butene, showing selectivities in the range of 78 to 86% and a *cis*/*trans*-2-butene ratio between 1.0 and 1.3. These results, which confirm the presence of acid sites, are in accordance with the conclusions from pyridine adsorption analyses. The evolution of the yields to the products of reaction and the amounts of Brønsted and Lewis acid sites (BAS and LAS) with the nominal Si/Al ratio are presented in Figs. 5 and 6, showing that the products of the reaction have the same evolution as the acid sites. These results also confirm the relation between the acid sites present on the surface of the prepared solids and the catalytic performance in the dehydration of 1-butanol.

4. Conclusions

This work reports the preparation of silica-alumina-pillared montmorillonites, structurally based on the aluminium Al_{13} polycation, by reaction with $Si(OC_2H_5)_4$.

Various methods have been applied, using the nitrogen adsorption data obtained at 77 K in order to analyse the microporous structure of silica-alumina-pillared montmorillonites. All methods describe satisfactorily the experimental results and qualitatively reproduce the micropore size distributions. The comparison of all distributions revealed that the samples show a bimodal micropore structure with a high structural heterogeneity.

The results of the characterisation of acidity of silica-alumina-pillared montmorillonites by pyridine adsorption followed by FTIR spectroscopy and the study of 1-butanol dehydration over the solids reveal that the surface of the samples shows mainly Lewis-type acidity.

Acknowledgments

Financial support by the Spanish Ministry of Science and Technology and FEDER (MAT2003-01255 and MAT2002-03526) is gratefully acknowledged.

References

[1] J.T. Kloprogge, J. Porous Mater. 5 (1998) 5.
[2] Z. Ding, J.T. Kloprogge, R.L. Frost, G.Q. Lu, H.Y. Zhu, J. Porous Mater. 8 (2001) 273.
[3] A. Gil, L.M. Gandía, M.A. Vicente, Catal. Rev.-Sci. Eng. 42 (2000) 145.
[4] R.S. Varma, Tetrahedron 58 (2002) 1235.
[5] P. Cool, E.F. Vansant, G. Poncelet, R.A. Schoonheydt, in: F. Schüth, K.S.W. Sing, J. Weitkamp (Eds.), Handbook of Porous Solids, Wiley–VCH, 2002, p. 1250.
[6] M. Sahimi, J. Chem. Phys. 92 (1990) 5107.
[7] M.S.A. Baksh, R.T. Yang, AIChE J. 38 (1992) 1357.
[8] L.S. Cheng, R.T. Yang, Chem. Eng. Sci. 49 (1994) 2599.
[9] H.T. Zhu, N. Maes, A. Molinard, E.F. Vansant, Micropor. Mater. 3 (1994) 235.
[10] A. Gil, P. Grange, Langmuir 13 (1997) 4483.
[11] L.J. Michot, F. Villiéras, J.-F. Lambert, L. Bergaoui, Y. Grillet, J.-L. Robert, J. Phys. Chem. B 102 (1998) 3466.
[12] J.P. Olivier, M.L. Occelli, J. Phys. Chem. B 105 (2001) 623.
[13] A. Gil, L.M. Gandía, Chem. Eng. Sci. 58 (2003) 3059.
[14] C.E. Salmas, A.K. Ladavos, S.P. Skaribas, P.J. Pomonis, G.P. Androutsopoulos, Langmuir 19 (2003) 8777.
[15] M.P. Atkins, European Patent Appl. WO 85/03015 (1985).
[16] M.L. Occelli, J. Mol. Catal. 35 (1986) 377.
[17] T.J. Pinnavaia, I.D. Johnson, US Patent 4,621,070 (1986).
[18] J. Sterte, J. Shabtai, Clays Clay Miner. 35 (1987) 429.
[19] I.D. Johnson, T.A. Werpy, T.J. Pinnavaia, J. Am. Chem. Soc. 110 (1988) 8545.
[20] D. Zhao, Y. Yang, X. Guo, Inorg. Chem. 31 (1992) 4727.
[21] G. Fetter, D. Tichit, P. Massiani, D. Dutartre, F. Figueras, Clays Clay Miner. 42 (1994) 161.
[22] G. Fetter, D. Tichit, L.C. de Menorval, F. Figueras, Appl. Catal. A 126 (1995) 165.
[23] A. Gil, G. Guiu, P. Grange, M. Montes, J. Phys. Chem. 99 (1995) 301.
[24] F. Figueras, Catal. Rev.-Sci. Eng. 30 (1988) 457.
[25] M.-Y. He, Z. Lin, E. Min, Catal. Today 2 (1988) 321.
[26] J.-F. Lambert, G. Poncelet, Topics Catal. 4 (1997) 43.
[27] A.N. Carvalho, A. Martins, J.M. Silva, J. Pires, H. Vasques, M. Brotas de Carvalho, Clays Clay Miner. 51 (2003) 340.
[28] S. Bodoardo, F. Figueras, E. Garrone, J. Catal. 147 (1994) 223.
[29] H. Auer, H. Hofmann, Appl. Catal. A 97 (1993) 23.
[30] S.M. Bradley, R.A. Kydd, J. Catal. 141 (1993) 239.
[31] M.L. Occelli, R.M. Tindwa, Clays Clay Miner. 31 (1983) 22.
[32] J.Y. Bottero, J.M. Cases, F. Fiessinger, J.E. Poirier, J. Phys. Chem. 84 (1980) 2933.
[33] S.M. Bradley, R.A. Kydd, R. Yamdagni, J. Chem. Soc., Dalton Trans. (1990) 2653.
[34] S.-I. Wada, K. Wada, J. Soil Sci. 31 (1980) 457.
[35] S.J. Gregg, K.S.W. Sing, Adsorption, Surface Area and Porosity, Academic Press, London, 1991.
[36] S.A. Korili, A. Gil, Adsorption 7 (2001) 249.
[37] L.M. Gandía, M.A. Vicente, A. Gil, Stud. Surf. Sci. Catal. 144 (2002) 585.
[38] A. Molinard, E.F. Vansant, Adsorption 1 (1995) 49.
[39] G. Horvath, K. Kawazoe, J. Chem. Eng. Jpn. 16 (1983) 470.
[40] A. Saito, H.C. Foley, AIChE J. 37 (1991) 429.
[41] A. Gil, P. Grange, Colloid Surf. A 113 (1996) 39.

[42] M. Jaroniec, K.P. Gadkaree, J. Choma, Colloid Surf. A 118 (1996) 203.
[43] D. Avnir, M. Jaroniec, Langmuir 5 (1989) 1431.
[44] A. Gil, G.Yu. Cherkashinin, S.A. Korili, J. Chem. Eng. Data 49 (2004) 639.
[45] M. Jaroniec, R. Madey, Physical Adsorption on Heterogeneous Solids, Elsevier, Amsterdam, 1988.
[46] P. Pfeifer, D. Avnir, J. Chem. Phys. 79 (1983) 3558.
[47] E.P. Parry, J. Catal. 2 (1963) 371.
[48] J. Datka, A.M. Turek, J.M. Jehng, I.E. Wachs, J. Catal. 135 (1992) 186.
[49] K. Jirátová, L. Beránex, Appl. Catal. 2 (1982) 125.
[50] P. Berteau, S. Ceckiewicz, B. Delmon, Appl. Catal. 31 (1987) 361.
[51] P. Berteau, B. Delmon, Catal. Today 5 (1989) 121.
[52] Y.F. Shen, A.N. Ko, P. Grange, Appl. Catal. 67 (1990) 93.
[53] P. Berteau, B. Delmon, J.-L. Dallons, A. Van Gysel, Appl. Catal. 70 (1991) 307.
[54] H.L. Del Castillo, P. Grange, Appl. Catal. 103 (1993) 23.
[55] F.M. Bautista, B. Delmon, Appl. Catal. A 130 (1995) 47.
[56] G. Guiu, P. Grange, J. Catal. 168 (1997) 463.
[57] J. Pires, A.P. Carvalho, P.R. Pereira, M. Brotas de Carvalho, React. Kinet. Catal. Lett. 65 (1998) 9.
[58] S. Delsarte, P. Grange, Appl. Catal. A 259 (2004) 269.
[59] Y. Fukuda, H. Hattori, K. Tanabe, Bull. Chem. Soc. Jpn. 51 (1978) 3150.
[60] Y. Nakano, T. Iizuka, T. Hattori, K. Tanabe, J. Catal. 57 (1979) 1.
[61] H. Noller, J.A. Lercher, H. Vinek, Mater. Chem. Phys. 18 (1988) 577.